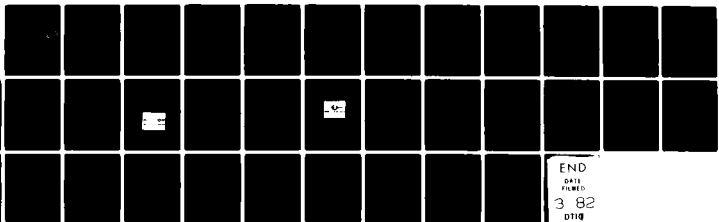


AD-A110 839

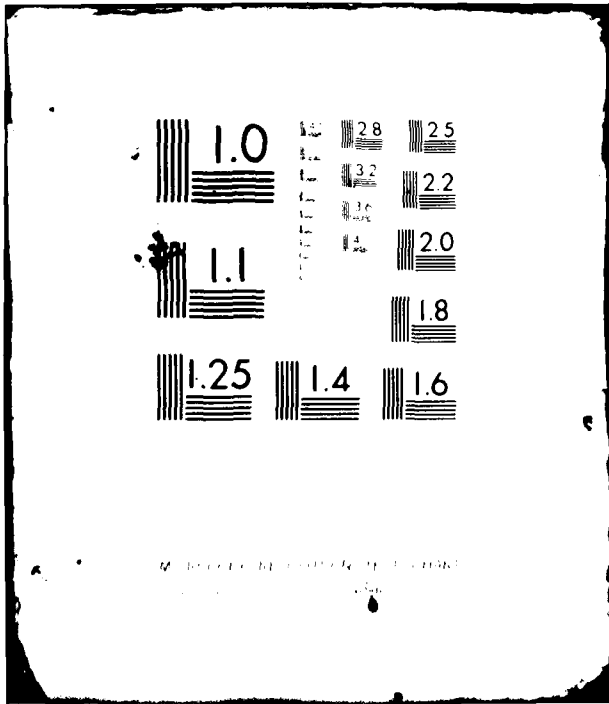
STANFORD UNIV CA EDWARD L GINZTON LAB OF PHYSICS F/6 20/2
ELASTIC DOMAIN WALL WAVES IN FERROELECTRIC CERAMICS AND SINGLE --ETC(U)
JAN 82 B A AULD N00014-79-C-0222
6L-3381 NL

UNCLASSIFIED

1 1
A. 08 0



END
DATA
FILMED
3 82
DTIC



LEVEL II

12

AD A110839

ELASTIC DOMAIN WALL WAVES IN FERROELECTRIC
CERAMICS AND SINGLE CRYSTALS

Annual Progress Report

1 February 1981 - 31 January 1982

Contract No. N00014-79-C-0222

DTIC
ELECTE
FEB 10 1982
S **D**
H

G.L. Report No. 3381

January 1982

Principal Investigator

B. A. Auld

DISTRIBUTION STATEMENT A
Approved for public release;
Distribution Unlimited

DTIC FILE COPY

Edward L. Ginzton Laboratory
W. W. Hansen Laboratories of Physics
Stanford University
Stanford, California 94305

82 227

UNCLASSIFIED

SECURITY CLASSIFICATION OF THIS PAGE (When Data Entered)

REPORT DOCUMENTATION PAGE		READ INSTRUCTIONS BEFORE COMPLETING FORM
1. REPORT NUMBER	2. GOVT ACCESSION NO. AD-1110839	3. RECIPIENT'S CATALOG NUMBER
4. TITLE (and Subtitle) ELASTIC DOMAIN WALL WAVES IN FERROELECTRIC CERAMICS AND SINGLE CRYSTALS		5. TYPE OF REPORT & PERIOD COVERED Annual Progress Report 1 Feb. 1981 - 31 Jan. 1982
7. AUTHOR(s) B. A. Auld		6. PERFORMING ORG. REPORT NUMBER G.L. Report No. 3381
9. PERFORMING ORGANIZATION NAME AND ADDRESS Edward L. Ginzton Laboratory W. W. Hansen Laboratories of Physics Stanford University, Stanford, CA 94305		8. CONTRACT OR GRANT NUMBER(s) N00014-79-C-0222
11. CONTROLLING OFFICE NAME AND ADDRESS Director, Metallurgy and Ceramics Program Office of Naval Research 800 N. Quincy St., Arlington, VA 22217		10. PROGRAM ELEMENT, PROJECT, TASK AREA & WORK UNIT NUMBERS
14. MONITORING AGENCY NAME & ADDRESS (if different from Controlling Office)		12. REPORT DATE January 1982
		13. NUMBER OF PAGES 35
		15. SECURITY CLASS. (of this report) UNCLASSIFIED
		15a. DECLASSIFICATION/DOWNGRADING SCHEDULE
16. DISTRIBUTION STATEMENT (of this Report) Approved for Public Release -- Distribution Unlimited		
17. DISTRIBUTION STATEMENT (of the abstract entered in Block 20, if different from Report)		
18. SUPPLEMENTARY NOTES		
19. KEY WORDS (Continue on reverse side if necessary and identify by block number) Piezoelectricity Transition Zone Ferroelectric Ceramics Pyroelectricity Differentially Poled Ceramic Domain Walls Heterodyne Laser Probe Interface Waves Counterpoling Elastic Waveguides Remanent Polarization		
20. ABSTRACT (Continue on reverse side if necessary and identify by block number) We have successfully launched and detected guided acoustic interface waves in both simulated domain wall structures and actual differentially poled ceramics. A heterodyne laser probe has been used to measure the acoustic field distributions associated with these waves. Remanent polarization and strain measurements have also been performed on differentially poled ceramic specimens. Composite resonators and interface waveguides are being characterized by laser probe techniques.		

DD FORM 1473
1 JAN 73EDITION OF 1 NOV 65 IS OBSOLETE
S/N 0102 LF 014-6801

UNCLASSIFIED

SECURITY CLASSIFICATION OF THIS PAGE (When Data Entered)

I. INTRODUCTION

In the past year, we have made further advances in the excitation and detection of elastic domain wall waves (also referred to as interface waves) in piezoelectric ceramics. Experiments have been conducted which demonstrate the existence of these waves in differentially poled ceramic structures, as well as in the simulated "glue bond" domain wall structure described in last year's report. An automated heterodyne laser probe scanning system has been utilized in the measurement and characterization of these guided interface waves. Using this experimental set-up, we were able to demonstrate that measured wave characteristics were in good agreement with theory. Conventional waveguide transmission measurements were also performed, and these also showed good agreement with theory.

In addition, we have performed experiments which elucidate some of the underlying principles governing the formation of transition zones in counterpoled ceramic structures. These experiments involved use of a laser beam to probe the polarization and strain distributions in a ceramic transition zone. The laser probe provides us with the means of simultaneously measuring polarization, strain, and elastic vibration profiles in the transition zone, and has proven to be a valuable tool in our research.

Currently, we are developing various prototype waveguide structures for potential device applications. These structures are compact, easy to fabricate, and support guided interface waves excited by edge bonded transducers. In addition, we have completed the first steps in a theoretical treatment of interface waves in bounded media, which will be important in thoroughly

understanding propagation behavior in our experimental waveguide structures. Finally, we are utilizing our laser probe in a collaboration with Walter Schulze of the Materials Research Laboratory at Penn State in a project involving the development of piezoelectric composite resonators for use as hydrophone transducers.

Accession For	<input checked="" type="checkbox"/>
NTIS (GPO)	<input type="checkbox"/>
DTIC TAB	<input type="checkbox"/>
Unannounced	<input type="checkbox"/>
Justification	
By	
Distribution/	
Availability Codes	
Dist	Special
A	



II. POLING AND COUNTERPOLING EXPERIMENTS

In the past year, we have continued our study of transition zones in counterpoled piezoelectric ceramics. As we have stated in past reports, these zones are characterized by a remanent polarization which undergoes a reversal within the zone. By measuring the spatial distribution of remanent polarization in the zone, we obtain a "polarization profile" which indicates the way that the ceramic responded to a local counterpoling field. A typical ceramic polarization profile is shown in Fig. 1(b). As one can see, the ceramic transition zone is quite "wide" relative to the crystal transition zone (or domain wall) shown in Fig. 1(a).

To manufacture a transition zone in a ceramic plate, one must first uniformly pole the entire sample in a given direction. One can then counterpole a portion of the plate by depositing a smaller local electrode, and applying poling voltage of the opposite polarity to this electrode. A boundary region, or transition zone, will result between regions of poled and counterpoled ceramic. The partial depoling observed in this region arises from: (1) intergranular stress accompanying polarization reversal in the contiguous counterpoled region, and to some extent (2) fringing fields emanating from the edge of the counterpoling electrode. As was noted in last year's report, axial strain on a poled (or counterpoled) ceramic can be on the order of 0.3% in relation to the depoled state.¹ Therefore, if we take an initially poled ceramic plate, and subject half of it to a counterpoling process (which takes the ceramic from a poled state through a depoled state to a counterpoled state), there can be as much as 0.3% difference in axial

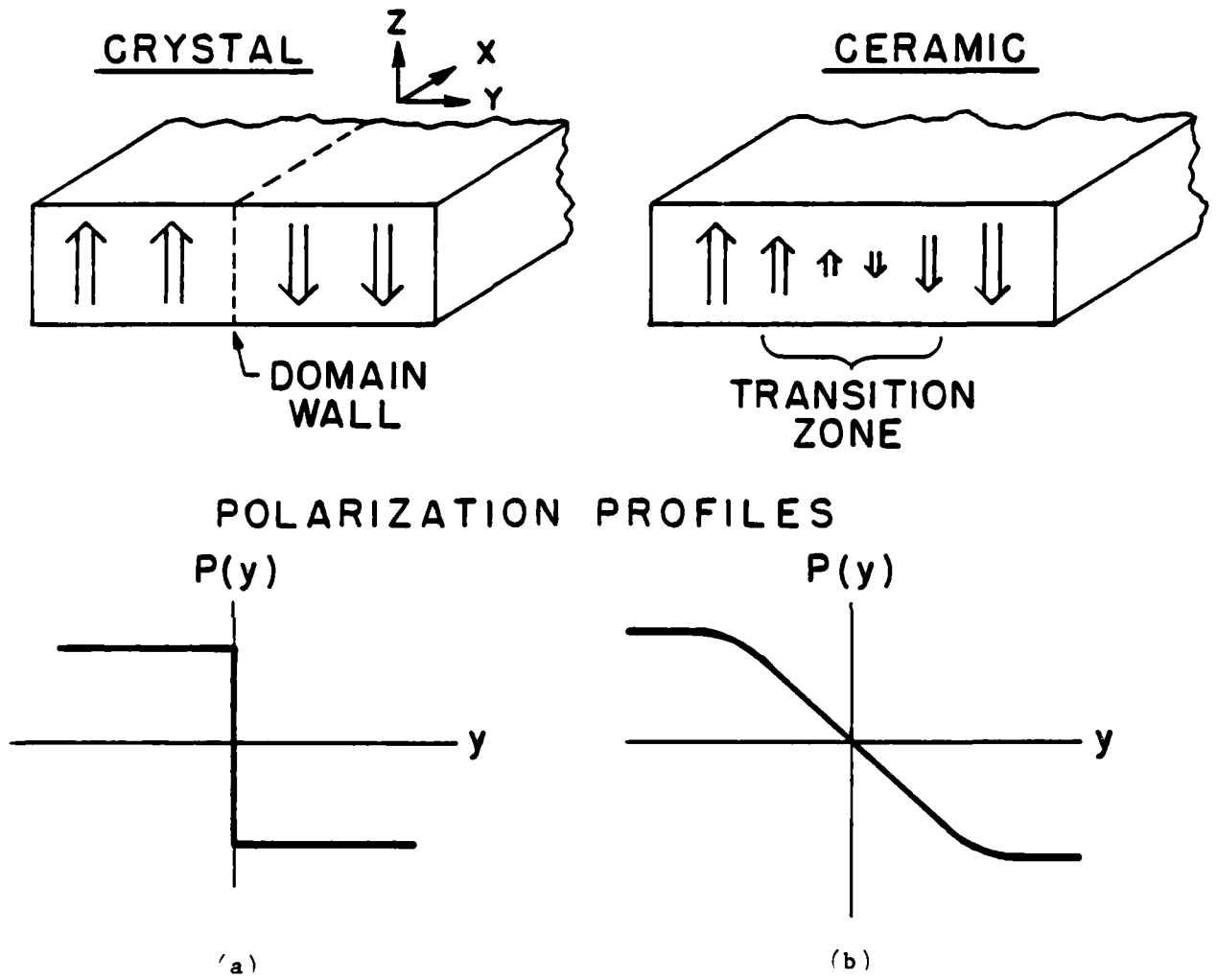
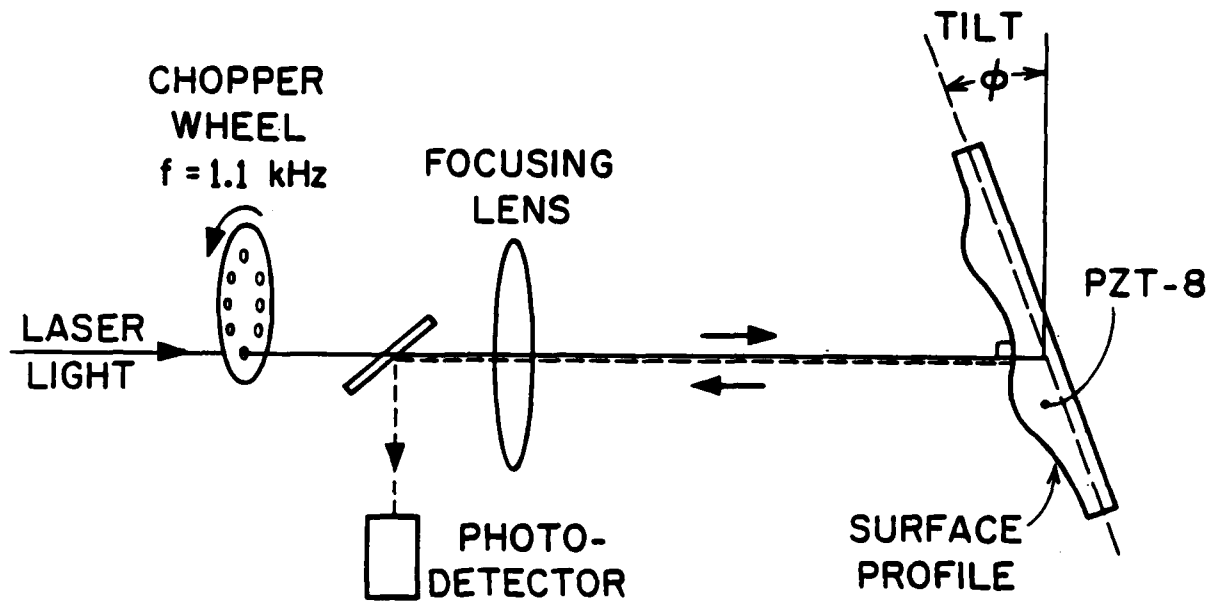


Fig. 1--Comparison of crystal and ceramic polarization profiles.

strain from one half of the plate to the other during the course of this process. In the final state, the counterpoled half has the same strain as the poled half, but the depoled ceramic in the transition zone retains the depoled strain state. This variation in remanent strain between poled and depoled ceramic gives rise to strong surface distortion in counterpoled ceramics. From measurements of this distortion in the vicinity of a transition zone, we can construct a strain profile of the region.

To make measurements of surface distortion in differentially poled ceramic plates, we used the laser system shown in Fig. 2. In our experiment, a ceramic plate was polished to a flatness of one optical wavelength and subsequently subjected to a differential poling treatment. The plate was then covered, top and bottom, with uniform gold electrodes and mounted to the tilt stage shown in Fig. 2. By measuring the tilt ϕ required to reflect a focused laser beam off the reflective surface and back into the photodetector, we obtain the slope of the surface at a given point. By repeating this measurement at various points along the ceramic plate, we can construct a surface profile of the plate, as shown at the bottom of Fig. 3.

In addition to the surface distortion measurement, the system in Fig. 2 is used to measure polarization profile in our ceramic plates. This measurement is accomplished by using a dynamic pyroelectric probe technique²⁻⁴ requiring a focused laser beam chopped at a low frequency. After insertion of the chopper wheel in the optical beam as shown in Fig. 2, the incident ray serves as a pulsed point source of heat which produces small changes in temperature at the focus. These small temperature fluctuations cause the spontaneous polarization at that point to vary, giving rise to an excess of free charge on the top and bottom electrodes.⁵ When these charges are allowed to flow through an external detection circuit, a pyroelectric current



LASER PROBE SYSTEM FOR SIMULTANEOUS
MEASUREMENT OF PYROELECTRIC CURRENT
AND SURFACE DISTORTION

Fig. 2--Laser probe system for simultaneous measurement
of pyroelectric current and surface distortion.

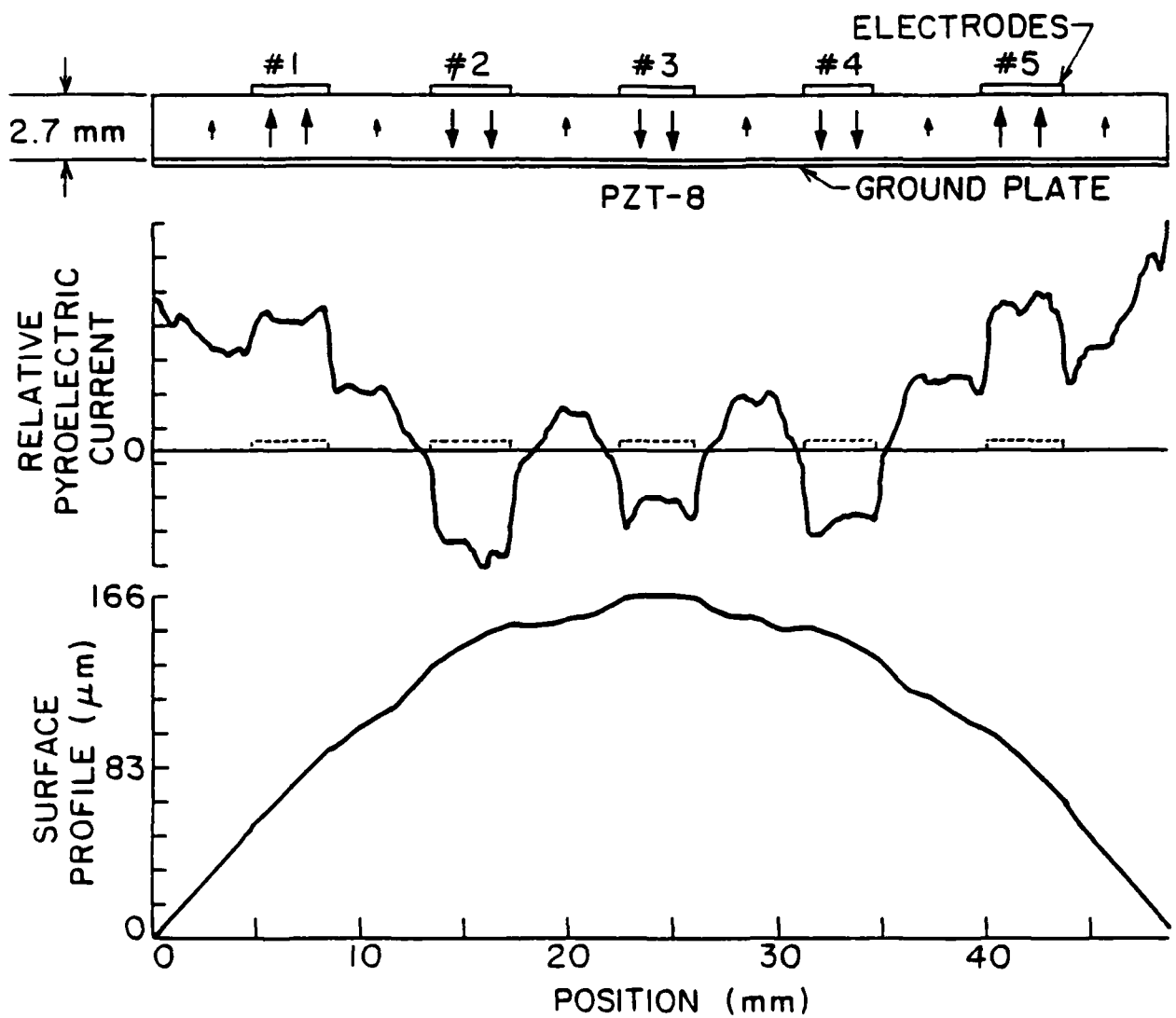


Fig. 3--Measured distributions of pyroelectric current and surface profile in a counterpoled sample of PZT-8 ceramic. The following poling scheme was used on the five electrodes: (1) poled for 1 minute, (2) counterpoled for 30 minutes, (3) counterpoled for 5 minutes, (4) counterpoled for 1 minute, (5) poled for 5 minutes.

can be measured having a magnitude proportional to the spontaneous polarization at that point.⁶ Consequently, by interrogating the surface of the sample point by point with the modulated laser beam, the spatial distribution of polarization can be measured. One such polarization profile is shown in Fig. 3 (middle). This measurement was made on a 50.0×16.3 mm rectangular plate of PZT-8 having a thickness of 2.7 mm. As shown schematically at the top of Fig. 3, five gold strip electrodes were deposited across the width of the rectangular ceramic plate, and a differential poling pattern was imposed on the initially uniformly-poled ceramic. Electrodes #2, #3, and #4 were counterpoled by application of + 5.55 kV to each electrode for 30 minutes, 5 minutes, and 1 minute, respectively. The original polarization of the ceramic was reinforced (not reversed) under electrodes #1 (for 1 minute) and #5 (for 5 minutes) by application of - 5.55 kV to each. All operations were carried out with the specimen immersed in a bath of peanut oil heated to a temperature $T \cong 147^{\circ}\text{C}$. After poling and counterpoling was completed, the five strip electrodes were etched away, and a full electrode was deposited on the top face.

The pyroelectric current profile (or polarization profile) shown in Fig. 3 demonstrates the effects of poling and counterpoling on our ceramic sample. The six regions at the edges of electrodes #2, #3, and #4 have polarization profiles exhibiting sign reversals, and hence qualify as transition zones. The effects of depolarization at points between the original strip electrodes are evident and are seen to extend over larger distances in the case of the longer counterpoling times. By way of illustration, a relatively "sharp" transition zone is observed around the electrode (#4) counterpoled for only 1 minute, whereas the 30 minute electrode (#2) has depoled ceramic as far out ~ 2 mm \pm on either edge. Furthermore, it is

apparent that 30 minute counterpoling effected a more thorough polarization reversal than did the other counterpolings. Finally, we note the shape of the polarization profile under each electrode. Except for the region under electrode #2 (and possibly #5) all of the regions have profiles that roughly resemble the electric field distribution under a poling electrode with edges. In other words, the ceramic becomes more thoroughly poled under the edges of the electrode, where the field lines are strongest. These patterns are the most recognizable in regions that were quickly poled or counterpoled. In regions treated for a longer time (#2: 30 mins.-counterpoled; #5: 30 mins.-poled), more complicated processes seem to be dictating the behavior.

Since our system has the ability to simultaneously measure polarization profile and surface distortion, it affords us with a natural means of studying the relation of remanent polarization and remanent strain in a ceramic. Comparison of the polarization profile along the surface with the actual surface distortion in Fig. 3 shows that the regions possessing strong remanent polarization relative to neighboring regions of weaker polarization "protrude" from the surface, standing out as convex "bumps." These "bumps" indicate regions possessing relatively large axial strains, and occur not only under all five electrodes, but also midway between these electrodes, in regions relatively unaffected by depoling forces. In the depoled regions, the remanent strain is significantly less than that in the surrounding material, and the ceramic surface assumes a concave shape. The overall warp of the entire piece is related to the asymmetry of the original poling structure, i.e., five strip electrodes on the top face and a single ground electrode on the bottom face. We believe that the lower half of the ceramic plate has more aligned (hence laterally strained) grains than the top half of the plate, causing a greater overall lateral contraction in the bottom.

This increased alignment in the bottom arises from the manner in which the field lines from a strip electrode spread before terminating on a ground plane.

Our laser probing system for determining polarization and strain profiles can also be used for the measurement of elastic vibration profiles in polished ceramic specimens. When an acousto-optic light modulator (i.e., Bragg cell) is placed in the beam as shown in Fig. 4, along with a few other suitably placed mirrors, our system becomes the heterodyne laser probe described by Ash and coworkers.⁷ A detailed description of our heterodyne system can be found in our last progress report.⁸ For demonstration purposes, the system was used to measure vibration amplitude as a function of position in our differentially poled ceramic structure, with the uniformly electroded sample driven at 380 kHz (Fig. 4).

The laser system which we have developed will also allow us to correlate measurements of polarization profiles with elastic vibration profiles of guided acoustic waves propagating in these zones. To facilitate measurements, our system is fully automated, using a minicomputer to translate the ceramic sample and collect data.

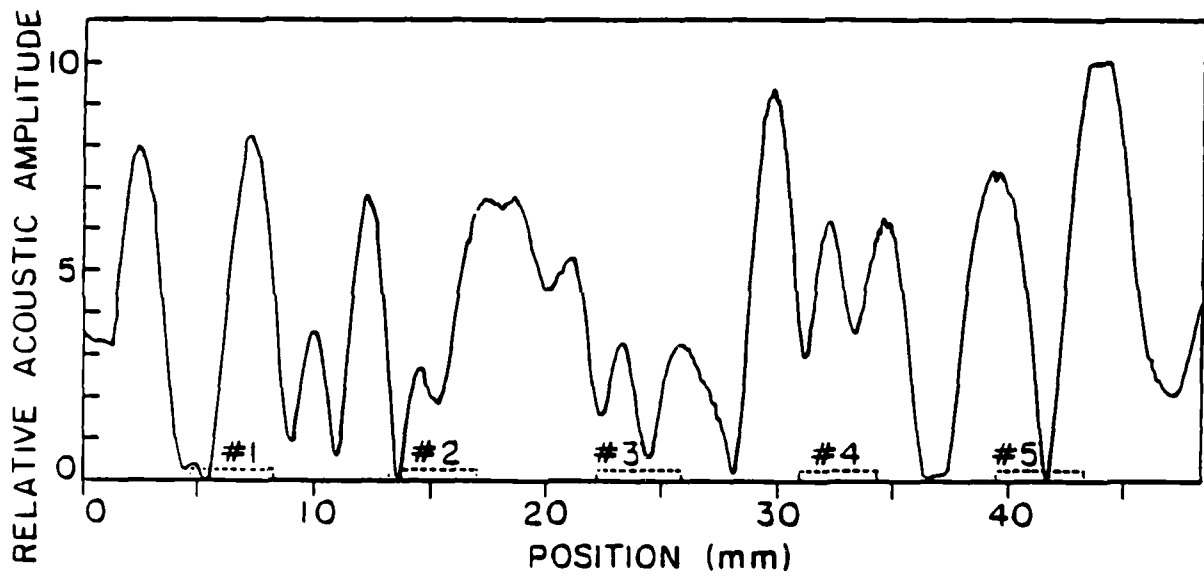
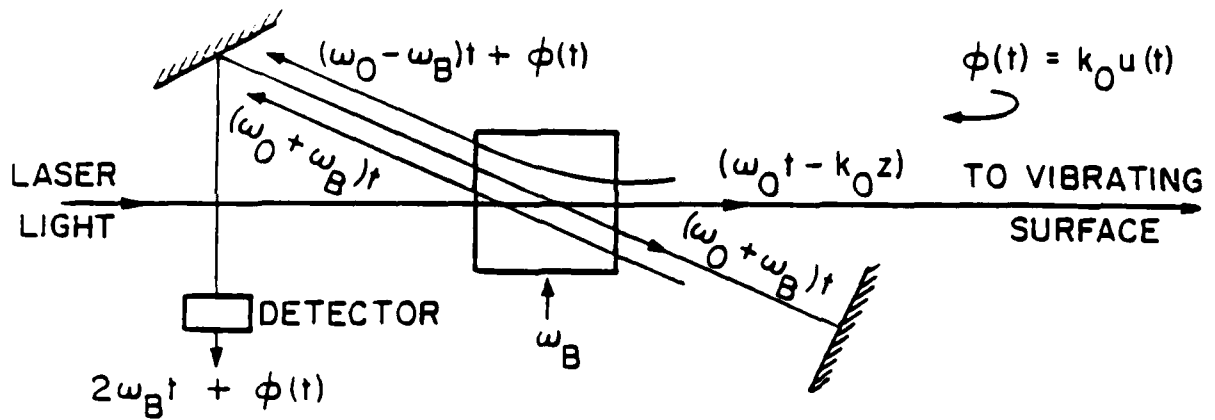


Fig. 4--Top: Schematic of laser probe system for measuring elastic vibration distributions in ceramic samples. Bottom: Measured distribution of elastic vibrations in the sample of Fig. 3 at 380 kHz.

III. WAVEGUIDE EXPERIMENTS

In last year's report, we described a ceramic waveguide structure consisting of two uniformly poled, thick PZT-8 bars, bonded together with their polar axes oriented anti-parallel to each other. This structure was intended to simulate the domain wall structure of Fig. 1(a), and support guided interface waves of the type predicted by Maerfeld and Tournois.⁹ These interface waves are shear-type, with their particle motion oriented along the poling axis and their propagation direction lying in a plane perpendicular to this axis. These characteristics are described schematically in Fig. 5. The guided wave is confined to the interface and propagates down the y-axis. We take k_y real and k_x imaginary, so that the wave is evanescent in the $\pm x$ -directions.

In a piezoelectric ceramic, this type of motion can be excited with interdigital transducers (IDT's) consisting of finger pairs parallel to the polar axis (z-axis) and periodic along the domain wall axis (y-axis). Transducers of this type (shown in Fig. 6) are situated in the plane of the interface, and the waveguide structure which results is shown at the top of Fig. 7. A structure having the same geometry and transducer placement as that in Fig. 7, but with two PZT-8 bars poled in the same direction, was also made. Comparing this structure with parallel polarization to the structure with anti-parallel polarization gives us a direct comparison of the effects of polarization reversal on wave propagation. At the time of last year's report, some preliminary pulse transmission measurements had been made on these "parallel" and "anti-parallel" ceramic glue-bond structures.

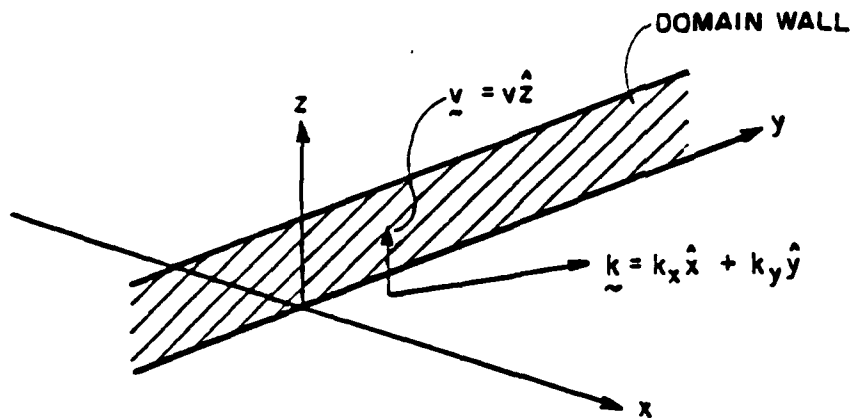
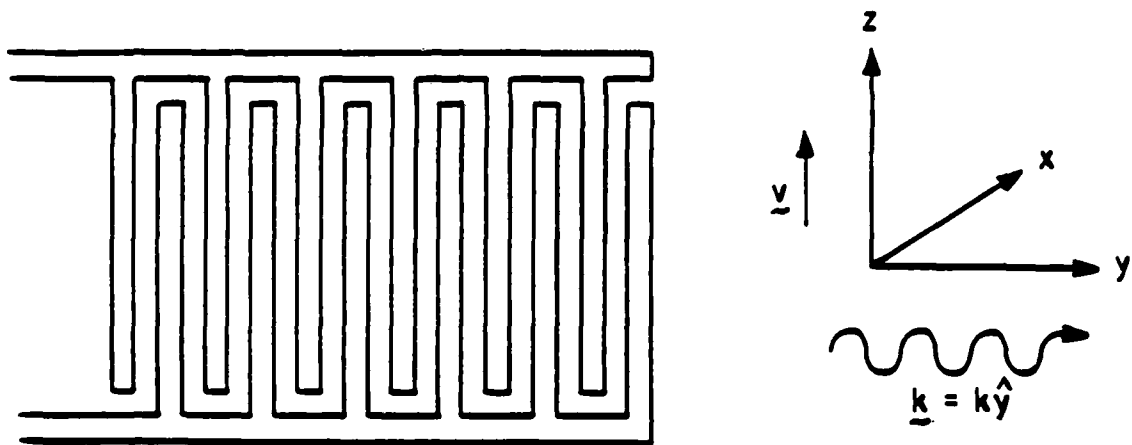


Fig. 5--Basic geometry for the study of shear-type interface waves in an infinite medium uniform in Z .



E-FIELDS LIE IN xy -PLANE.
PARTICLE MOTION POLARIZED
ALONG z -AXIS.

Fig. 6--Interdigital transducer used in the excitation of shear-type interface waves.

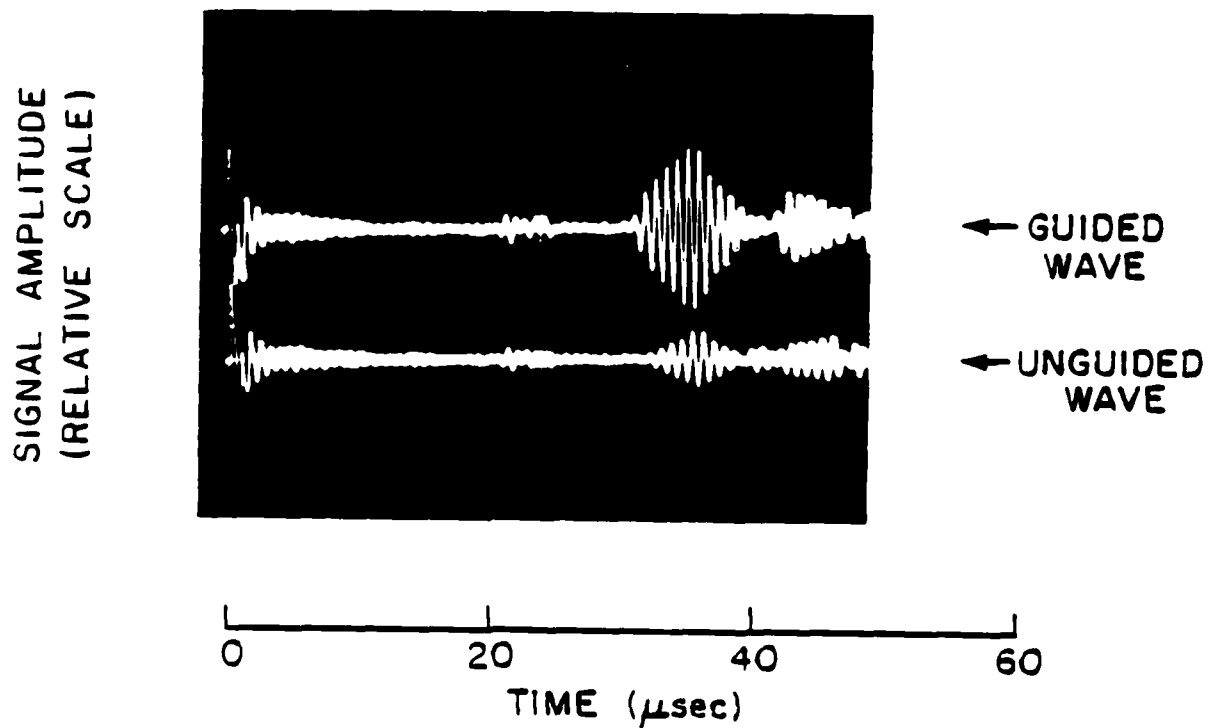
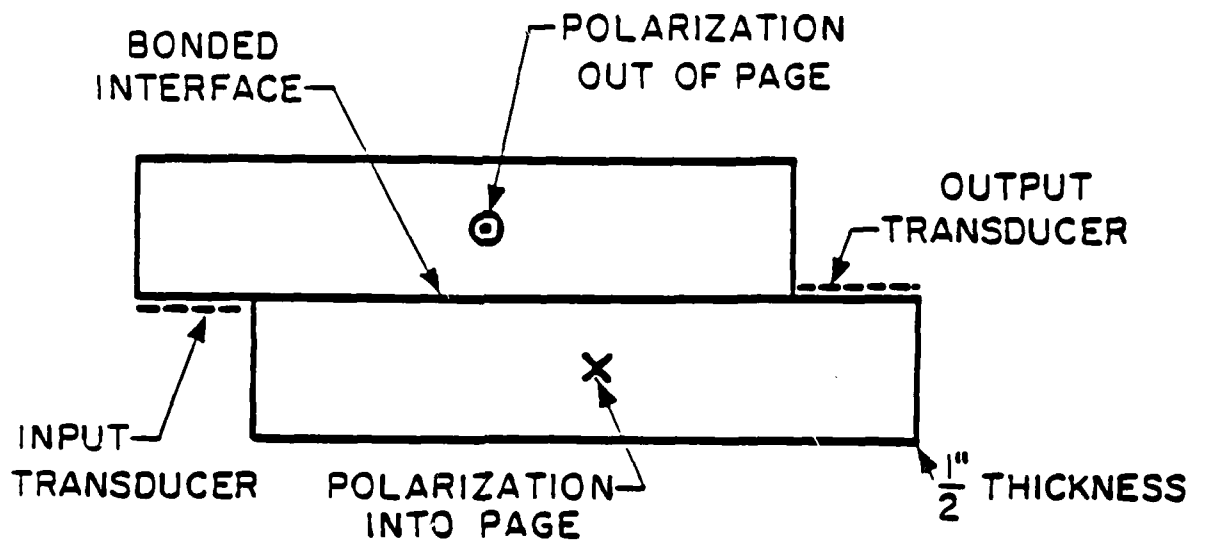


Fig. 7--Top: Ceramic waveguide structure for interface wave transmission experiments. Bottom: Pulse transmission measurements at $f = 1.15$ MHz comparing propagation in the waveguide structure (shown at top) with propagation in a control structure (having the same polarization in both bars).

Results indicating the presence of a guided wave are seen in Fig. 7. The top trace shows transmission in the structure having polarization reversal, and the bottom trace represents transmission in the control sample with no reversal.

This year, cw transmission measurements, along with some further pulse measurements, were made on the glue-bond structures. In the cw experiments, the input transducer of the waveguide was driven with a sinusoidal waveform, and the relative phase and amplitude of the signal at the output transducer were measured. By measuring these quantities as a function of frequency, we were able to obtain additional confirmation of interface waves in the structure, and excellent estimates of phase and group velocity. Since the input and output transducers were located in the plane of the interface, we expected to observe a transmission amplitude in the "anti-parallel" structure that would be significantly larger than the "parallel" structure transmission amplitude at certain frequencies. These frequencies would correspond to the points where the interface wave was efficiently driven by the input transducer, or, in other words, where the periodicity of the transducer matched that of the guided interface wave. Therefore, by knowing the periodicity of the transducer, and multiplying by the measured frequency at these transmission peaks, we could easily determine the phase velocity of the interface wave.

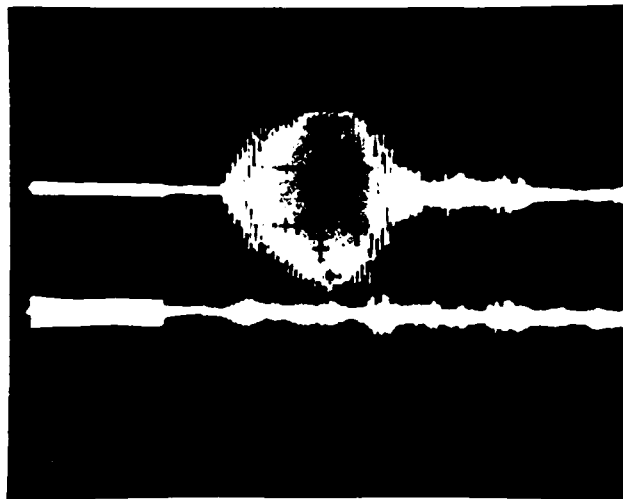
Additional evidence supporting the existence of guiding in our structures involved the complicated plate resonance behavior observed over most of the frequency range. At frequencies where interface waves were not excited, the transducers in both structures generated unguided bulk waves which propagated outward, interacting with the edges of the waveguide structure. Therefore, resonances associated with the structure dimensions

could be expected to appear at these frequencies. On the other hand, when interface waves were efficiently excited, the acoustic energy was mainly confined to the interface, away from the plate edges, and the usual plate resonance behavior was not observed.

We noticed optimal transmission of the interface wave in the "anti-parallel" glue-bond structure in the range 1.10 to 1.13 MHz. The IDT fingers were spaced by $\lambda/2$ where $\lambda = 2.032$ mm. Therefore, the phase velocity of the wave was computed to lie somewhere in the range 2.23 to 2.30 mm/ μ sec. The theoretically computed value for PZT-8 is 2.27 mm/ μ sec, in good agreement with our results. We also observed excellent interface transmission at the third harmonic of the IDT. Transmission in this range peaked at $f = 3.4$ MHz, giving us a value for phase velocity in good agreement with theory. By working at 3.4 MHz, most of the unguided bulk shear waves are launched into the substrate at an angle to the interface. At lower frequencies, these bulk waves travel closer to the interface, making measurements of the interface wave more difficult. Hence, at 3.4 MHz, transmission of unguided bulk waves was significantly reduced, and the presence of interface guiding could be observed only in the "anti-parallel" structure. This guiding is clearly shown in the pulse transmission measurement of Fig. 8. From our cw measurements, the presence of polarization reversal in the structure enhanced transmission by 10 to 20 dB in the frequency ranges corresponding to interface wave generation.

Group velocities were calculated from cw transmission data by measuring the slope of the phase vs. frequency curve. This slope is inversely proportional to the group velocity. Values ranging from 2.3 to 2.5 mm/ μ sec were obtained for the interface wave group velocity.

SIGNAL AMPLITUDE
(RELATIVE SCALE)



← GUIDED
WAVE

← UNGUIDED
WAVE

0 40 80 120
TIME (μ sec)

Fig. 8--Pulse transmission at $f = 3.4$ MHz comparing waveguide structure with control structure.

IV. LASER PROBE MEASUREMENTS OF GUIDED INTERFACE WAVES

The heterodyne laser probe affords us with an excellent means of determining the acoustic field distribution associated with an interface wave. By polishing the top face of the ceramic ~~sample~~ (the face perpendicular to the interface and poling axes) we can ~~see~~ view the waveguide structure as shown in Fig. 9, measuring both the wave's ~~phase~~ velocity and transverse acoustic amplitude profile. A sequence of these transverse profiles is shown in Fig. 10 for an interface wave propagating along the glue-bond structure of Fig. 7, driven at a cw frequency of $f = 1.37$ MHz. Referenced to this structure, the left-hand side of these profiles corresponds to the upper PZT bar and the right-hand side to the lower PZT bar. These scans were made at various points along the interface, with the upper scan being the closest to the input transducer, and the lower scan being the most distant. We see that the interface wave retains its basic shape as it propagates down the guide, possessing a profile which closely fits the transverse evanescent field variation predicted by Maerfeld and Tournois.⁹ In Fig. 11, typical transverse profiles taken at three different frequencies on the glue-bond structure are displayed. As expected, the wave is more tightly bound to the interface at higher frequencies. Similar scans carried out on the "parallel" glue-bond structure showed no wave confined to the interface, and demonstrated that the glue-bond itself performed no role in the wave guiding.

The phase velocity and dispersion characteristics of the interface wave were measured by scanning along the length of the guide. Large standing wave patterns were observed along the guide, indicating strong reflection of the

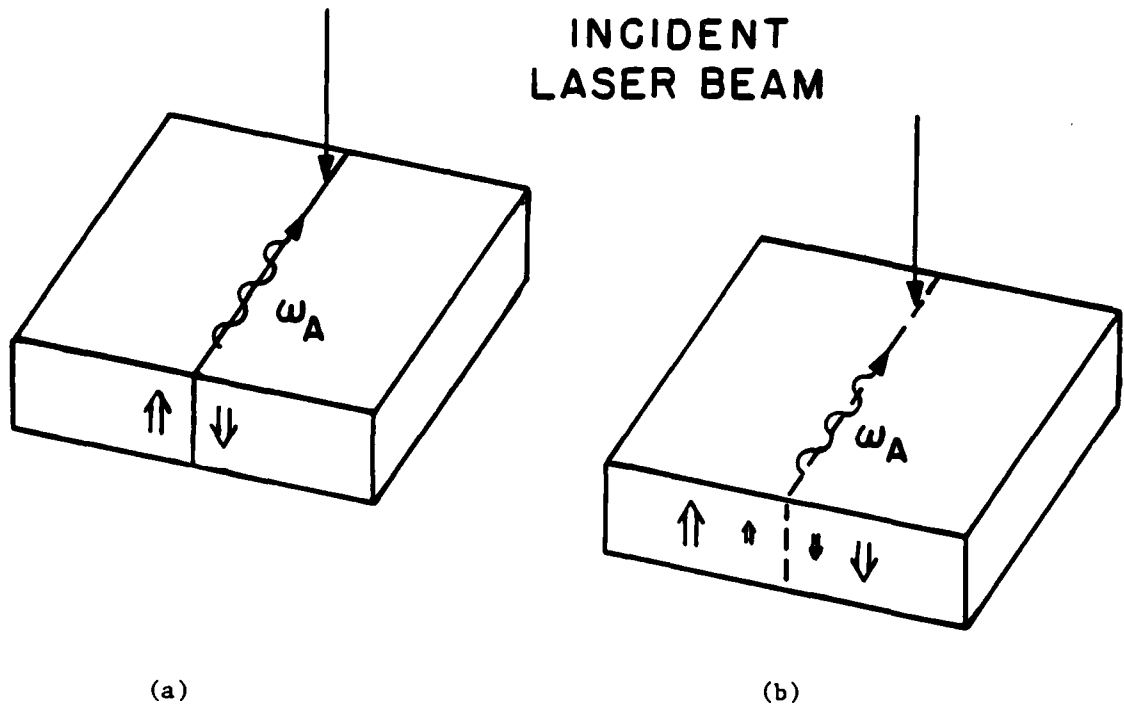


Fig. 9--Measurement of interface waves in (a) domain walls and (b) ceramic transition zones using heterodyne laser probe.

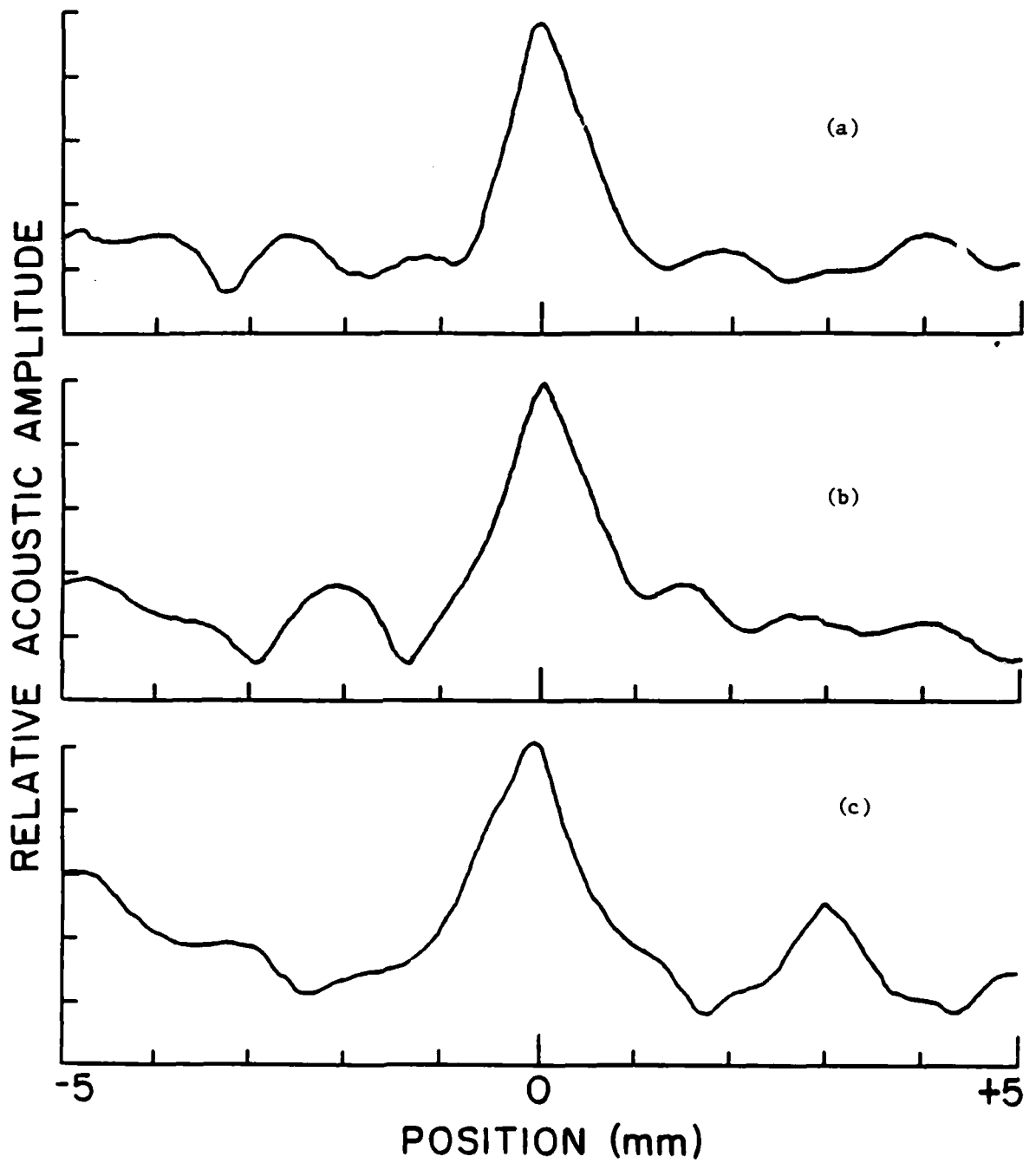


Fig. 10--Interface wave on glue-bond structure ($f = 1.37$ MHz).
(a) $x = 15.65$ mm, (b) $x = 42.65$ mm, (c) $x = 52.45$ mm.

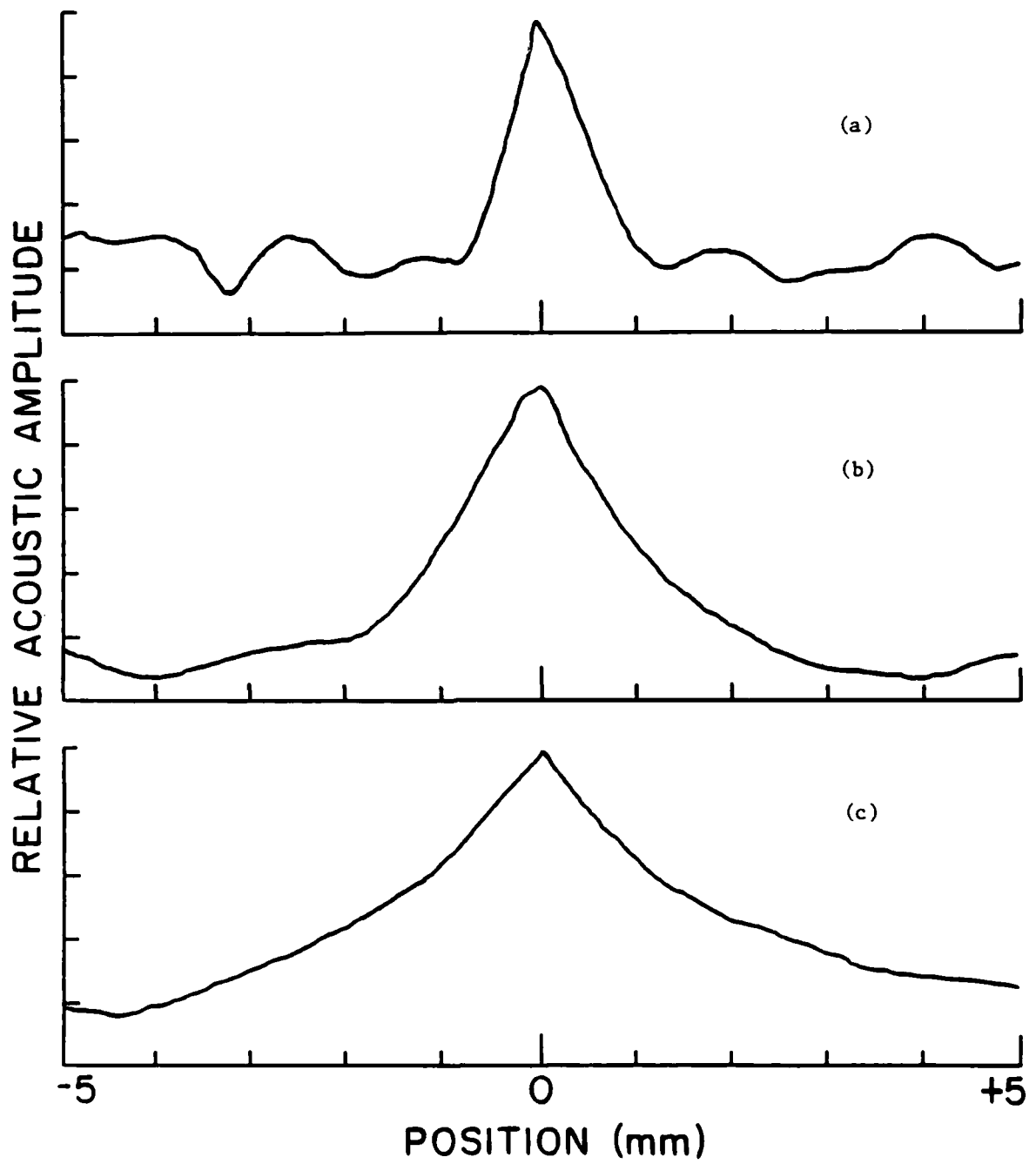


Fig. 11--Interface wave on glue-bond structure at various frequencies. (a) $f = 1.37$ MHz, (b) $f = 0.84$ MHz, (c) $f = 0.66$ MHz.

interface wave from the plate edge (we would expect this from a z-polarized motion reflected from a face or edge parallel to the z-axis). This strong conversion of forward traveling interface waves into backward traveling interface waves upon reflection from an edge should prove to be a useful property for the construction of resonators. From the standing wave patterns, we were able to measure the interface wave number β and hence compute phase velocity. Data taken in this manner from 660 kHz to 1.37 MHz indicated that β scaled fairly linearly with frequency. Phase velocities measured in this frequency interval ranged from 2.24 to 2.32 mm/ μ sec, in good agreement with theory.

In addition to the glue-bond guide, we used the laser probe to study guided acoustic waves in differentially poled ceramics. In such structures, there can exist a shear-type guided wave which is confined to the transition zone and propagates with a phase velocity lower than that of a Maerfeld-Tournois domain wall wave. In our first year's progress report, we extended the theory of the Maerfeld-Tournois wave to the case where remanent polarization and material constants were allowed to vary smoothly as functions of position in a transition zone of finite width.¹⁰ We have shown that the transition zone will support additional higher order waveguide modes as it is widened with respect to acoustic wavelength. As frequency is decreased, these higher order modes will become unguided when their phase velocities match that of the Maerfeld-Tournois interface wave. The lowest order mode exists at all frequencies, and actually becomes the Maerfeld-Tournois wave in the limit $f \rightarrow 0$ (or, equivalently, $\lambda \rightarrow \infty$, where even wide transition zones appear narrow to the long wavelength acoustic wave).

Because of the depoled ceramic in the interior of a transition zone, efficient piezoelectric excitation of an acoustic interface must take place

on the periphery of the zone. One possible means of exciting such a wave is shown in Fig. 12. A 1/8" thick PZT-8 (4" x 2") was counterpoled as shown in the figure to form a transition zone along the length of the sample. Acoustic waves were launched into the transition region by means of two interdigital transducers placed on the surface of the plate so as to straddle the interface. These IDT's generated electric driving fields in the plane normal to the poling axis, so that shear-type interface motion (coupled through k_{15}) could be induced. The IDT fingers were spaced by $\lambda/2$ ($\lambda = 2.03$ mm), and were 2λ in length. Therefore, with a Rayleigh range of only 4λ , unguided bulk waves generated by the transducers would rapidly spread, making the effect of transition zone guiding more evident.

By driving the transducers out of phase, a particle displacement field symmetric about the interface was launched along the guide, in an attempt to excite waveguide modes of even symmetry. Using the laser probe as before, we performed scans of the elastic vibration distribution in the differentially poled plate. Transverse scans of the ceramic transition zone at different frequencies are shown in Fig. 13, each taken roughly 50 mm from the input transducers. In these acoustic amplitude profiles, zero marks the edge of the original counterpoling electrode and the depoled region extends about 1.5 mm to the right of zero. The guiding afforded by the transition zone is clearly evident.

We also attempted to launch an odd waveguide mode by driving the transducers in-phase. Some suggestive amplitude profiles are shown in Fig. 14. As the phase profile has not been displayed here, it must be pointed out that the two central humps are oscillating out of phase with respect to each other, representing a particle motion which is basically antisymmetric. We found that it was difficult to find "odd mode" profiles of this variety

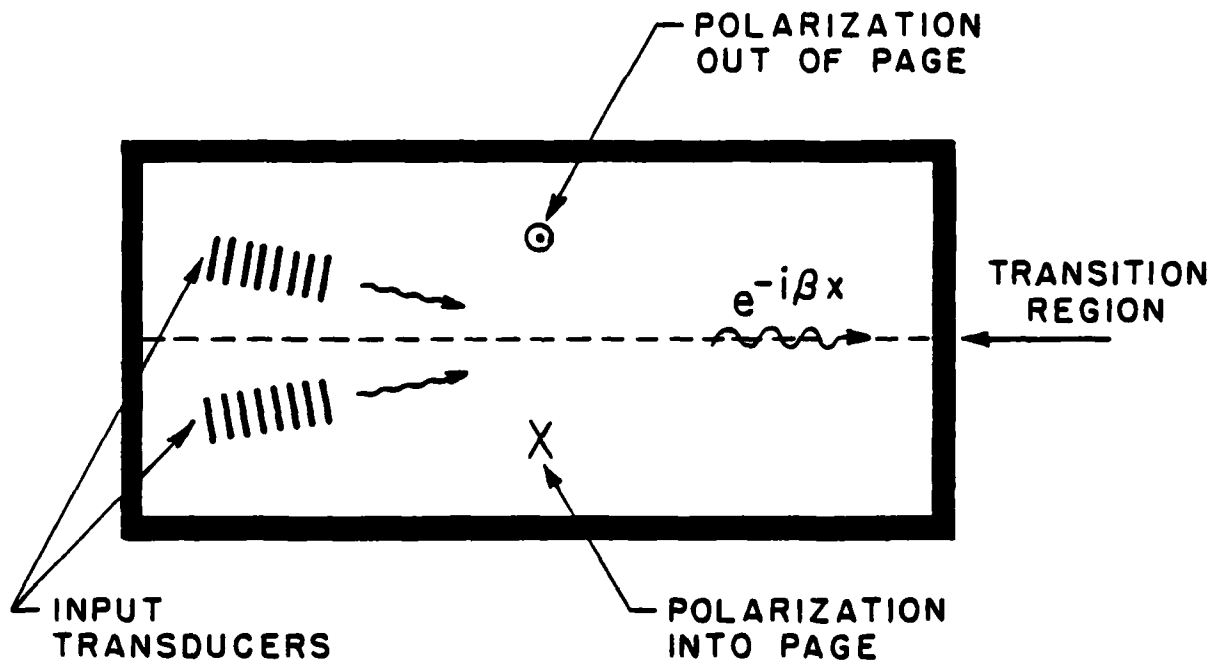


Fig. 12--Transducer configuration used to excite interface modes in a differentially poled ceramic plate.

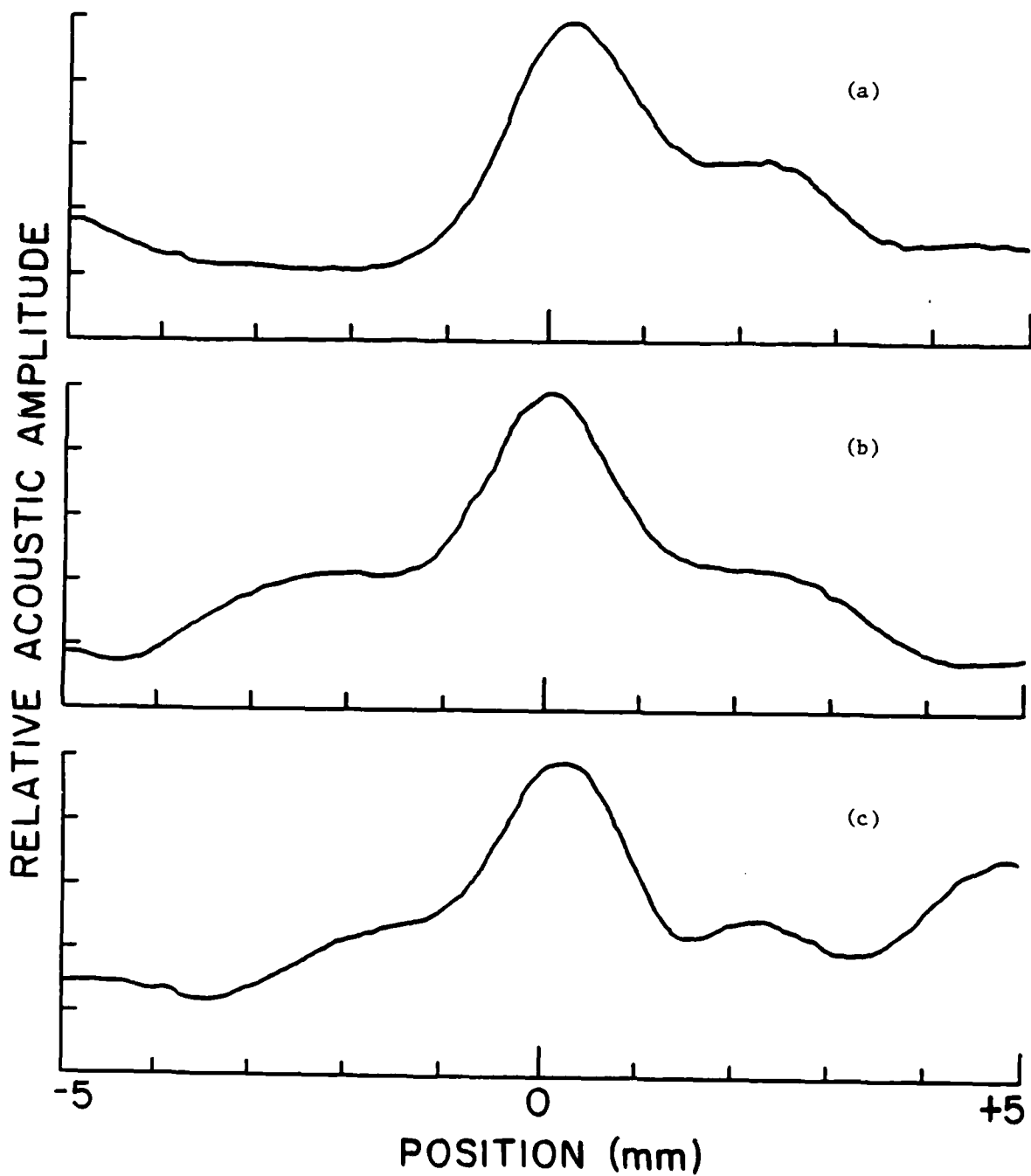


Fig. 13--Interface waves propagating in a ceramic transition zone driven by a symmetric strain field. Distance from input transducer ≈ 50 mm. (a) $f = 930$ kHz, (b) $f = 860$ kHz, (c) $f = 780$ kHz.

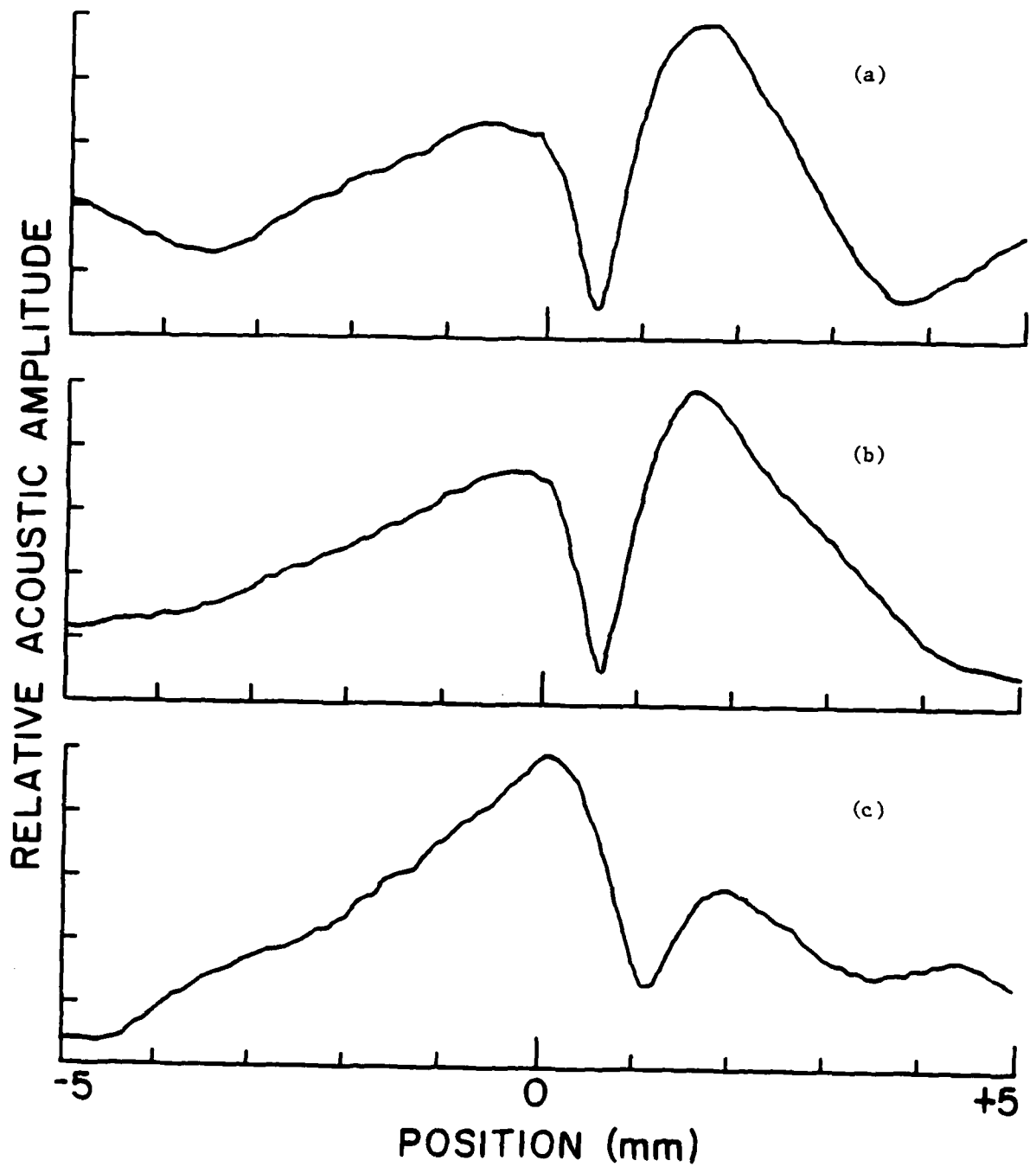


Fig. 14--Interface waves propagating in a ceramic transition zone driven by an antisymmetric strain field. Distance from input transducer ≈ 50 mm. (a) $f = 1000$ kHz, (b) $f = 960$ kHz, (c) $f = 930$ kHz.

much below 930 kHz, possibly due to the waveguide cut-off. In fact, profiles made of waves launched in this fashion below 930 kHz more closely resembled a weakly excited symmetric guided mode. Conversion of this sort (from odd excitation field to even waveguide mode) is conceivable in transition zones having asymmetric polarization profiles (such as ours). Phase velocities for both modes were measured in the interval 2.0 to 2.3 mm/ μ sec, which is the range between the unstiffened bulk shear velocity and the Maerfeld-Tournois velocity.

Finally, it must be noted that the heterodyne laser probe system is fully automated. A laboratory computer both runs the experiments and collects the data. To facilitate quick measurements of vibration profiles without concern for surface distortion measurements, we have inserted a microscope objective into the optical path to focus the incident beam onto the ceramic. As alignment is critical in the laser probe, the presence of a short focal length microscope lens in front of the sample desensitizes the system to misalignment. As shown in Fig. 15, a sample misaligned or warped at an angle θ to the horizontal results in a reflected beam displaced by a distance d from true alignment. This misalignment distance can be minimized by choosing focal length f to be small (as in a microscope objective). By making this choice of lens, we have been able to perform automated scans across highly warped ceramic surfaces without need for sample realignment.

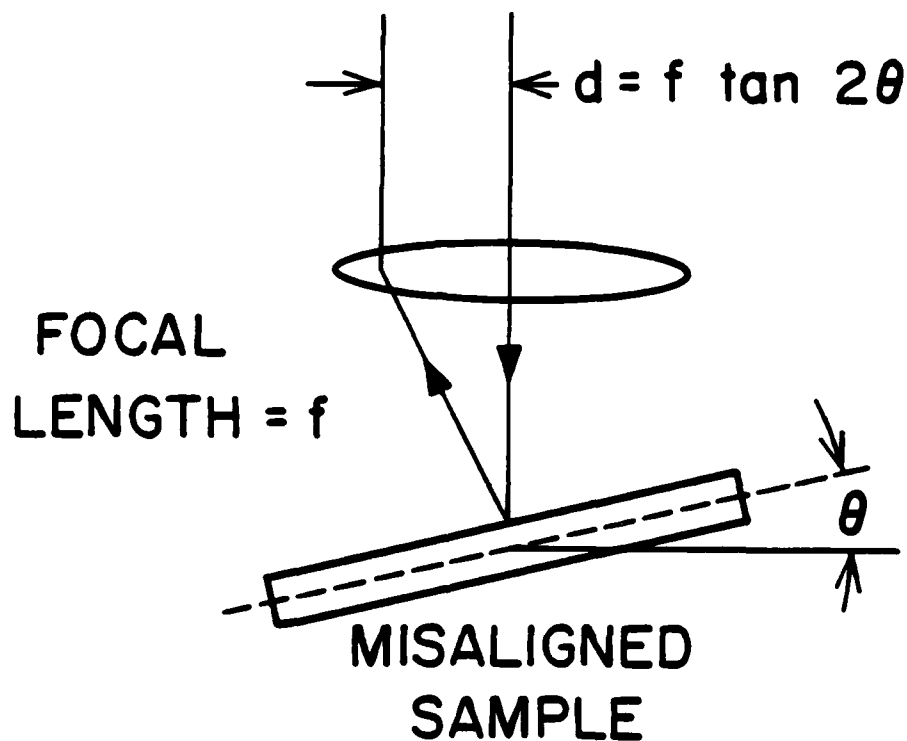


Fig. 15--The laser probe system can be made sensitive or insensitive to misalignment by a suitable choice of focal length f . For measurements of remanent strain profile (using tilt micrometers), we would like the alignment of the system to be very sensitive to changes in surface slope, hence large f . If we are not interested in this strain profile, and wish to make elastic vibration measurements quickly and easily (where alignment is critical), we use a lens of very small focal length (e.g., a microscope objective).

V. PLATE WAVE CALCULATIONS

We have demonstrated experimentally that interface waves exist in bounded media (e.g., a ceramic plate). Unfortunately, our theory up to this point has only treated the interface or zone which is infinite in two dimensions (i.e., filling the entire y - z plane in Fig. 5). To realize this infinite medium condition experimentally we have been required to use ceramic plates with thicknesses many times larger than the relative acoustic wavelength. This requirement has proven to be an unfortunate limitation, especially when one considers the many interesting ceramics available only in small sizes. Therefore, in the past year we have formulated a theoretical treatment of the interface wave in a bounded medium. In particular, we have turned our attention to the case of the thin domain wall or glue-bond interface in a ceramic plate with poling axes perpendicular to the plate faces. Our method basically consists of constructing the interface wave as a linear superposition of piezoelectric plate waves. At this point, we are still developing some of the computer programs, and no results are yet available. We believe that this theory will allow us to build and understand interface waveguides operating in the low frequency or thin plate regime.

VI. APPLICATION OF LASER PROBE TO STUDY OF COMPOSITE RESONATORS

Following a recent trip to the Materials Research Laboratory at Penn State, we have begun a collaboration with Walter Schulze in the study of 3:1 connected PZT:epoxy composites. These composites consist of a set of PZT rods aligned in an epoxy resin matrix and driven in a longitudinal mode configuration. The Penn State group has been fabricating these materials for use in hydrophone devices, and d_{hg_h} products (figure of merit) of up to $4,000 \times 10^{-12} \text{ m}^2/\text{N}$ have been demonstrated.¹¹

To understand the effects of various design parameters on hydrophone performance, it is desirable to understand the way in which these devices vibrate. Our program with Penn State involves the measurement of these resonator vibrations using the heterodyne laser probe. The probe is used to scan the face of the resonator, obtaining vibration profiles associated with the embedded matrix of PZT rods. By measuring profiles as a function of frequency, we hope to determine the manner in which the individual rods interact with each other and the epoxy resin around them. This work is currently in progress.

VII. CONCLUSION

In summary, we have successfully launched and detected guided acoustic interface waves in both simulated domain wall structures and actual differentially poled ceramics. From pulse and cw transmission measurements, we have demonstrated that the presence of 180° polarization reversal across a thin glue-bond interface accounts for a 10 to 20 dB increase in transmission along a 3-inch guide. Interface guidance has also been systematically studied using a heterodyne laser probe, and results indicate that the "thin wall" interface wave possesses the phase velocity and acoustic field distribution predicted by Maerfeld and Tournois. Our laser probe has also been used to measure the acoustic field distributions in a differentially poled ceramic. A guided acoustic wave confined to the ceramic transition zone is observed, with properties analogous to the Maerfeld-Tournois wave. In addition, the laser probe has been adapted to perform simultaneous measurements of remanent polarization and strain profiles in differentially poled ceramics.

To make interface waves a practical tool in research and technology, our goal has been the development of an efficient yet simple means of launching a pure interface wave into a practical ceramic waveguide structure. To this end, we are currently constructing a series of both glue-bond structures and differentially poled ceramic structures having various dimensions and compositions. For this generation of waveguides, we have elected to use the edge bonded transducer to launch interface waves into the guide. From previous use in non-destructive testing applications, these transducers

have been shown to have sufficiently wide bandwidth for good pulse operation. Moreover, they are easy to fabricate, and can be used interchangeably from waveguide to waveguide.

VIII. REFERENCES

1. D. Berlincourt and H. H. A. Krueger, J. Appl. Phys. 30, 1804 (1959).
2. A. G. Chynoweth, Phys. Rev. 102, 705 (1956).
3. A. G. Chynoweth, J. Appl. Phys. 27, 78 (1956).
4. A. Hadni, J. M. Bassia, X. Gerbaux, and R. Thomas, Appl. Optics 15, 2150 (1976).
5. M. E. Lines and A. M. Glass, Principles and Applications of Ferroelectrics and Related Materials (Oxford: Clarendon Press, 1977), pp. 141-148.
6. S. T. Liu and J. D. Zook, Ferroelectrics 7, 171 (1974).
7. R. M. De La Rue, R. F. Humphreys, I. M. Mason, and E. A. Ash, Proc. IEEE 119, 117 (1972).
8. B. A. Auld, "Elastic Domain Wall Waves in Ferroelectric Ceramics and Single Crystals," Ginzton Laboratory Report No. 3314, Stanford University, Stanford, California (September 1981).
9. C. Maerfeld and P. Tournois, Appl. Phys. Lett. 19, 117 (1971).
10. B. A. Auld, "Elastic Domain Wall Waves in Ferroelectric Ceramics and Single Crystals," Ginzton Laboratory Report No. 3076, Stanford University, Stanford, California (January 1980).
11. L. E. Cross, R. E. Newnham, G. R. Barsch, and J. V. Biggers, "Targeted Basic Studies of Ferroelectric and Ferroelastic Materials for Piezoelectric Transducer Applications," Annual Report, Office of Naval Research, Washington, D.C. (December 1980).

IX. PRESENTATIONS

1. B. A. Auld and H. A. Kunkel, "Laser Probe Measurements of Material Properties and Elastic Vibration Distributions in Counterpoled Ceramics," presented at the 5th International Meeting on Ferroelectricity (August 1981).
2. H. A. Kunkel and B. A. Auld, "Laser Probe Investigation of Guided Acoustic Interface Waves in Differentially Poled Ceramics," presented at the IEEE Ultrasonics Symposium, Chicago (October 1981).

X. PUBLICATIONS

1. B. A. Auld and H. A. Kunkel, "Laser Probe Measurements of Material Properties and Elastic Vibration Distributions in Counterpoled Ceramics," *Ferroelectrics* 38, 971-974 (1981).
2. H. A. Kunkel and B. A. Auld, "Laser Probe Investigation of Guided Acoustic Interface Waves in Differentially Poled Ceramics," 1981 Ultrasonics Symposium Proceedings (to be published).

XI. VISITS

H. A. Kunkel attended the Penn State Materials Research Laboratory review presentation on Targeted Basic Studies of Ferroelectric and Ferroelastic Materials for Piezoelectric Transducer Applications (November 1981).

**DA
FILM**